

# Generation and replication of continuous-variable quadripartite cluster and Greenberger-Horne-Zeilinger states in four chains of superconducting transmission line resonators

Zhen Li, Sheng-li Ma, Zhi-peng Yang, Ai-ping Fang, Pen-bo Li, Shao-yan Gao, and Fu-li Li\*

*Shaanxi Province Key Laboratory of Quantum Information and Quantum Optoelectronic Devices and Department of Applied Physics, School of Science, Xi'an Jiaotong University, Xi'an 710049, People's Republic of China*

(Received 13 December 2015; published 4 April 2016)

We consider a system consisting of four independent chains of coupled single-mode superconducting transmission line resonators and a gap-tunable qubit. When the first four resonators of the chains are coupled to the qubit properly driven by multicolor fields, we show that the resonators can be prepared in continuous-variable quadripartite cluster states via the decay of the qubit to its ground state. Moreover, the resulting cluster states can be replicated in the other resonators in column via the nearest-neighbor swapping interaction of the resonators. This means that one can generate a set of cluster states, each of which involves the four resonators from the different chains. By a similar protocol, we show that the generation and replication of continuous-variable quadripartite Greenberger-Horne-Zeilinger states in the chains of the resonators can be achieved. The numerical simulation shows that the present scheme is realizable in current accessible on-chip quantum circuit experiments. The present result may have a potential application for the realization of a large-scale one-way quantum computation.

DOI: [10.1103/PhysRevA.93.042305](https://doi.org/10.1103/PhysRevA.93.042305)

## I. INTRODUCTION

Quantum entanglement is one of the most fascinating features of quantum mechanics and is an indispensable resource for implementing various quantum information protocols, such as quantum teleportation [1,2] and quantum dense coding [3,4]. The generation of quantum entangled states has always been a central topic in both fundamental research of quantum mechanics and applications of quantum information and quantum computing. During the past two decades, great progress on this subject has been made. Entangled states of discrete variables such as spin, polarization, and energy levels have successfully been generated and widely used in experiments [5–11]. Because of high efficiency in the generation, manipulation, and detection of phase-quadrature amplitude components of optical fields, on the other hand, considerable effort has also been concentrated on producing continuous-variable (CV) entanglement [12–21]. Multipartite entanglement has more sophisticated quantum correlations compared with bipartite entanglement. Multimode CV entangled states are crucial resources for constructing quantum communication networks and implementing quantum computation. Therefore, particular interest has been directed at generating multicomponent CV entangled states, such as the CV Greenberger-Horne-Zeilinger (GHZ) state [22–25] and CV cluster state [26–30]. Among various types of multipartite CV entangled states, CV cluster states [26] may be more interesting since one-way quantum computation [31–33] can be realized based on CV cluster states. The experimental generation of CV cluster states and GHZ states has been achieved in linear optics systems [24]. By means of a pair of nondegenerate optical parametric amplifiers and linear optics, the target states can be engineered by linear optical transformation of squeezed light with certain phase relations. In addition, a scheme was also proposed to create CV cluster states based on the collective excitation of four distinct atomic ensembles located inside a ring cavity [28].

Superconducting circuits [34–38], which can be designed and constructed on demand and possess the advantages of integration and scaling on a chip, are promising candidates for studying fundamental quantum physics and implementing quantum information protocols. In particular, circuit quantum electrodynamics (QED), an on-the-chip counterpart of cavity QED systems, has attracted great interest. This system provides an unprecedented level of tunability, flexibility, and scalability in the implementation of the strong-coupling limit and allows rapid quantum-state manipulation. Thus, it becomes a very interesting issue how to generate various entangled states and implement scalable quantum computation in circuit QED systems. In fact, a system composed of one-dimensional coplanar waveguide resonators dispersively coupled by a single superconducting qubit or qutrit has been investigated for generating entangled states and implementing quantum information transfer [39–41]. The deterministic generation of NOON entangled states in two superconducting resonators coupled by a phase qubit has been demonstrated experimentally [42]. In recent work [43], a multicavity system in which each cavity contains many superconducting qubits and all the cavities are coupled to a single superconducting qubit was studied for the generation of GHZ states [43].

In this paper we investigate the generation and replication of quadripartite CV clusters in a circuit QED system. The system under consideration consists of a gap-tunable superconducting qubit and four chains of linearly coupled superconducting transmission line resonators. The beginning four resonators of the chains are simultaneously coupled to the qubit. With the periodic modulation of the transition frequency of the qubit, we can simultaneously realize both the parametric down-conversion-like and the beam-splitter-like interactions between the qubit and the resonators. It is shown that quadripartite CV cluster states of the cavity fields of the resonators can be engineered by employing the energy relaxation of the qubit. More interestingly, we show that the resulting CV cluster states of the first four resonators can be replicated among the whole resonator chains. The present

\*fli@mail.xjtu.edu.cn

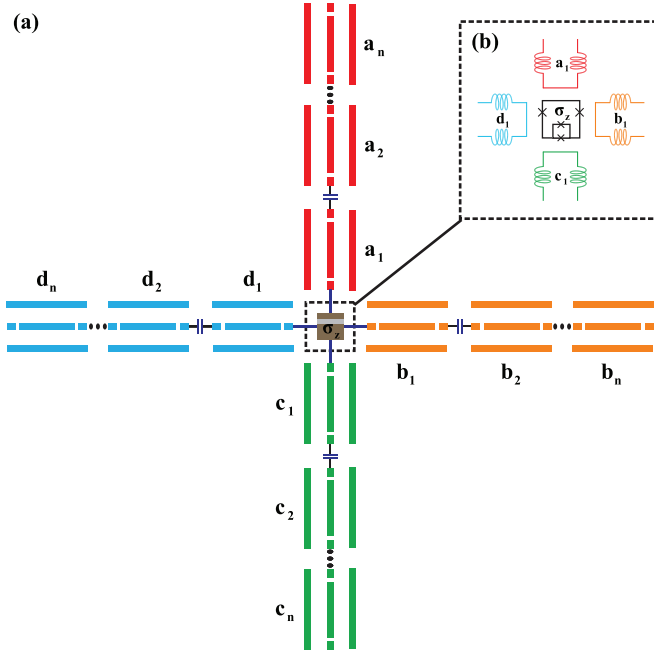


FIG. 1. Schematic of a circuit cavity electromechanical system composed of four independent superconducting transmission line resonator arrays and a gap-tunable superconducting qubit. The enlarged inset represents a possible coupling way of the qubit with the first four resonators.

result may have a potential application for the realization of a large-scale one-way quantum computation based on quantum on-chip circuits. Using a similar approach, we also show that quadripartite CV GHZ states of the cavity fields can also be generated and replicated in the whole resonator chains.

The paper is organized as follows. In Sec. II, the model is introduced. In Sec. III, the four kinds of orthogonal combination modes of the fields of the resonators are introduced for linear, square, and T-shape cluster states. The effective Hamiltonian for the generation of single-mode squeezed states is derived. The generation of the cluster states through four steps is investigated in detail. In Sec. IV, the generation of the GHZ states through four steps is discussed in detail. In Sec. V, a brief discussion and summary are given.

## II. MODEL

The system under consideration is composed of four independent arrays  $a$ ,  $b$ ,  $c$ , and  $d$ , each of which consists of  $N$  identical superconducting transmission line resonators, linked with each other through capacitors. The first four resonators of the chains are coupled together via a gap-tunable superconducting qubit [39,44]. The model is schematically depicted in Fig. 1.

The Hamiltonian of the whole system is ( $\hbar = 1$ )

$$H = H_0 + H_1 + H_2 + H_{\text{drive}}, \quad (1)$$

where

$$H_0 = \frac{\omega_0}{2} \sigma_z + \sum_{n=1}^N (\omega_a a_n^\dagger a_n + \omega_b b_n^\dagger b_n + \omega_c c_n^\dagger c_n + \omega_d d_n^\dagger d_n), \quad (2)$$

$$H_1 = (\sigma_+ + \sigma_-)[g_a(a_1 + a_1^\dagger) + g_b(b_1 + b_1^\dagger) + g_c(c_1^\dagger + c_1) + g_d(d_1^\dagger + d_1)], \quad (3)$$

$$H_2 = \sum_{n=1}^{N-1} J(a_n^\dagger a_{n+1} + b_n^\dagger b_{n+1} + c_n^\dagger c_{n+1} + d_n^\dagger d_{n+1} + \text{H.c.}), \quad (4)$$

$$H_{\text{drive}} = -\sigma_z \sum_k [\xi_{+,k} \omega_{+,k} \cos(\omega_{+,k} t + \phi_{+,k}) + \xi_{-,k} \omega_{-,k} \cos(\omega_{-,k} t + \phi_{-,k})], \quad (5)$$

with  $k = a, b, c, d$  characterizing the four independent resonator chains. Here  $H_0$  represents the free energies of the qubit and the four arrays of  $N$  identical superconducting transmission line resonators, respectively,  $\omega_0$  is the static energy gap between the ground state  $|g\rangle$  and the excited state  $|e\rangle$  of the qubit,  $\sigma_z = |e\rangle\langle e| - |g\rangle\langle g|$ ,  $a_n(b_n, c_n, d_n)$  are the annihilation operators for photons in the  $n$ th resonator of the chain  $a(b, c, d)$ , and  $\omega_a(\omega_b, \omega_c, \omega_d)$  is the resonant frequency of the resonators of the chain  $a(b, c, d)$ . The interaction between the qubit and the first four resonators is given by  $H_1$ , in which  $g_a(g_b, g_c, g_d)$  is the coupling strength between the qubit and the cavity mode  $a_1(b_1, c_1, d_1)$  and the spin-flip operator  $\sigma_+, \sigma_- = |e\rangle\langle g|, |g\rangle\langle e|$ , and  $H_2$  describes the energy exchange between resonators via the nearest-neighbor linear coupling with the same strength  $J$ .

In addition, we apply a four-pair  $\sigma_z$  driving to the qubit whose transition frequency is periodically modulated in time. The energy levels of the qubit and its driving frequencies are shown in Fig. 2. Such a manipulation is described by the time-dependent Hamiltonian  $H_d$  [45], in which  $\omega_{\pm,k}$  ( $k = a, b, c, d$ ) are the driving frequencies,  $\xi_{\pm,k}$  are the ratios between the driving amplitudes and driving frequencies, and  $\phi_{\pm,k}$  are the tunable phases. In principle, the modulating process can be implemented with various types of gap-tunable superconducting qubits, such as flux [46], charge [47], or transmon [48] qubits. For instance, we can adopt four Josephson junctions, i.e., the smallest two Josephson junctions with the coupling energy smaller than that of the other two junctions by a factor  $\alpha$ , forming a low-inductance dc superconducting quantum interference device (SQUID) loop. The  $\sigma_z$  driving process can be realized by applying time-dependent external magnetic fields penetrating the SQUID loop [49].

The dynamics of the whole system is governed by the master equation

$$\frac{d\rho}{dt} = -i[H, \rho] + \frac{\Gamma}{2} D[\sigma_-]\rho, \quad (6)$$

where  $\rho$  is the time-evolution density operator of the whole system and  $D[\sigma_-]\rho = (2\sigma_- \rho \sigma_+ - \rho \sigma_+ \sigma_- - \sigma_+ \sigma_- \rho)$  is the standard Lindblad operator. Here we only consider the decay

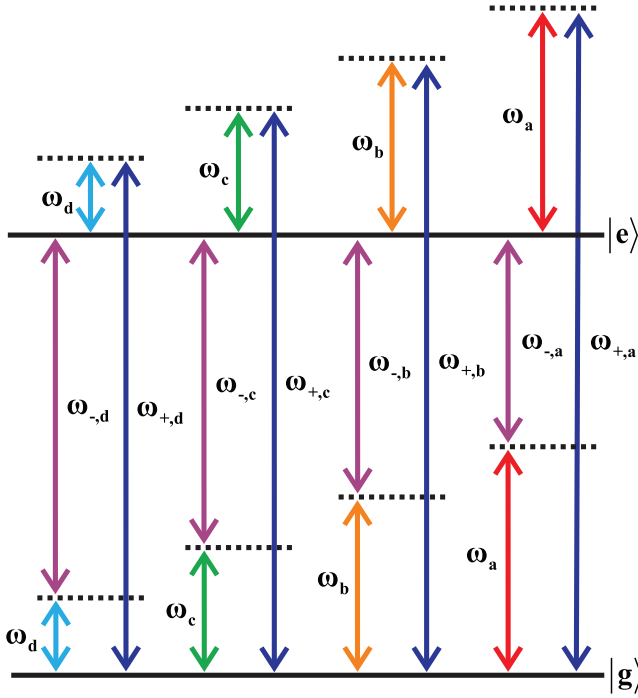


FIG. 2. Schematic of sideband transitions of the superconducting qubit.

process of the qubit with the rate  $\Gamma$  and ignore other possible dissipative processes such as photon loss of the resonators since the decay rate of superconducting transmission line resonators is typically in the sub-MHz range and much smaller than that of the qubit [50].

### III. GENERATION AND REPLICATION OF QUADRIPARTITE CONTINUOUS-VARIABLE CLUSTER STATES

For four entities, there are three different cluster states: a linear cluster state, square cluster state, and T-shape cluster state, as shown in Fig. 3. The variances of the quadrature amplitudes of the fields in CV quadripartite cluster states obey the conditions [27]

$$V\left(P_j - \sum_{i \in N_j} X_i\right) \rightarrow 0, \quad j = 1, 2, 3, 4, \quad (7)$$

in the limit of infinite squeezing. In Eq. (7),  $X_j$  and  $P_j$  are the phase-quadrature amplitude operators of the  $j$ th mode of the fields according to the definition  $a_j = (X_j - iP_j)/\sqrt{2}$ , where  $a_j$  is the annihilation operator of the  $j$ th mode, and the modes

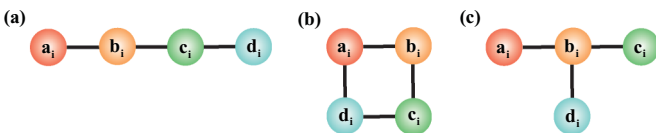


FIG. 3. Structure of CV quadripartite cluster states: (a) linear cluster, (b) square cluster state, and (c) T-shape cluster state.

$i \in N_j$  in the summation are all the nearest neighbors  $N_j$  of the mode  $j$ .

For a linear cluster state of the four modes  $a_n, b_n, c_n, d_n$  of the  $n$ th resonators of the arrays in Fig. 3(a), we consider the amplitude combinations

$$\begin{aligned} P_{a_n} - X_{b_n} &= -[i(a_n - a_n^\dagger) + (b_n + b_n^\dagger)]/\sqrt{2}, \\ P_{b_n} - X_{a_n} - X_{c_n} &= -[i(b_n - b_n^\dagger) + (a_n + a_n^\dagger) \\ &\quad + (c_n + c_n^\dagger)]/\sqrt{2}, \\ P_{c_n} - X_{b_n} - X_{d_n} &= -[i(c_n - c_n^\dagger) + (b_n + b_n^\dagger) \\ &\quad + (d_n + d_n^\dagger)]/\sqrt{2}, \\ P_{d_n} - X_{c_n} &= -[i(d_n - d_n^\dagger) + (c_n + c_n^\dagger)]/\sqrt{2}. \end{aligned} \quad (8)$$

In terms of the four combined-mode annihilation operators defined as

$$\begin{pmatrix} A_n \\ B_n \\ C_n \\ D_n \end{pmatrix} = \begin{pmatrix} -\frac{i}{\sqrt{2}} & -\frac{1}{\sqrt{2}} & 0 & 0 \\ -\frac{1}{\sqrt{2}} & -\frac{i}{\sqrt{2}} & -\frac{1}{\sqrt{2}} & 0 \\ 0 & -\frac{1}{\sqrt{2}} & -\frac{i}{\sqrt{2}} & -\frac{1}{\sqrt{2}} \\ 0 & 0 & -\frac{1}{\sqrt{2}} & -\frac{i}{\sqrt{2}} \end{pmatrix} \begin{pmatrix} a_n \\ b_n \\ c_n \\ d_n \end{pmatrix} \quad (9)$$

and their Hermitian conjugation operators, Eqs. (8) can be rewritten as

$$\begin{aligned} P_{a_n} - X_{b_n} &= A_n^\dagger + A_n, \\ P_{b_n} - X_{a_n} - X_{c_n} &= B_n^\dagger + B_n, \\ P_{c_n} - X_{b_n} - X_{d_n} &= C_n^\dagger + C_n, \\ P_{d_n} - X_{c_n} &= D_n^\dagger + D_n. \end{aligned} \quad (10)$$

It now becomes clear that the condition (7) can be satisfied if each of those combined modes is in an amplitude squeezed state. Since the combined modes  $A_n, B_n, C_n, D_n$  are not orthogonal to each other, however, one cannot independently prepare each of the combined modes in an amplitude squeezed state. Thus, we orthogonalize the transformation matrix in Eq. (9) and redefine the four combined modes

$$\begin{pmatrix} \bar{A}_n \\ \bar{B}_n \\ \bar{C}_n \\ \bar{D}_n \end{pmatrix} = \begin{pmatrix} -\frac{i}{\sqrt{2}} & -\frac{1}{\sqrt{2}} & 0 & 0 \\ -\frac{1}{\sqrt{3}} & -\frac{i}{\sqrt{3}} & -\frac{1}{\sqrt{3}} & 0 \\ \frac{i}{\sqrt{10}} & -\frac{1}{\sqrt{10}} & -i\sqrt{\frac{2}{5}} & -\sqrt{\frac{2}{5}} \\ \frac{1}{\sqrt{15}} & \frac{i}{\sqrt{15}} & -\frac{2}{\sqrt{15}} & -i\sqrt{\frac{3}{5}} \end{pmatrix} \begin{pmatrix} a_n \\ b_n \\ c_n \\ d_n \end{pmatrix} \quad (11)$$

In terms of these annihilation operators of the new combined modes and their Hermitian conjugates, we have

$$\begin{aligned} V(P_{a_n} - X_{b_n}) &= V(\bar{A}_n + \bar{A}_n^\dagger), \\ V(P_{b_n} - X_{a_n} - X_{c_n}) &= \frac{3}{2}V(\bar{B}_n + \bar{B}_n^\dagger), \\ V(P_{c_n} - X_{b_n} - X_{d_n}) &= \frac{1}{4}V(\bar{A}_n + \bar{A}_n^\dagger) + \frac{5}{4}V(\bar{C}_n + \bar{C}_n^\dagger), \\ V(P_{d_n} - X_{c_n}) &= \frac{1}{6}V(\bar{B}_n + \bar{B}_n^\dagger) + \frac{5}{6}V(\bar{D}_n + \bar{D}_n^\dagger). \end{aligned} \quad (12)$$

Since the combined modes  $\bar{A}_n, \bar{B}_n, \bar{C}_n, \bar{D}_n$  are independent, one can separately prepare each of the modes in an amplitude squeezed state. In this way, the condition (7) will be satisfied and the original modes  $a_n, b_n, c_n, d_n$  are in a linear cluster state. Therefore, the generation of a linear cluster state of the four

modes  $a_n, b_n, c_n, d_n$  is equivalent to the preparation of four amplitude squeezed states for the combined modes as defined in Eq. (11).

For a square cluster state of the four modes  $a_n, b_n, c_n, d_n$  of the  $n$ th resonators of the arrays as shown in Fig. 3(b), we consider the amplitude combinations

$$\begin{aligned}
P_{a_n} - X_{b_n} - X_{d_n} &= -[i(a_n - a_n^\dagger) + (b_n + b_n^\dagger) \\
&\quad + (d_n + d_n^\dagger)]/\sqrt{2}, \\
P_{b_n} - X_{a_n} - X_{c_n} &= -[i(b_n - b_n^\dagger) + (a_n + a_n^\dagger) \\
&\quad + (c_n + c_n^\dagger)]/\sqrt{2}, \\
P_{c_n} - X_{b_n} - X_{d_n} &= -[i(c_n - c_n^\dagger) + (b_n + b_n^\dagger) \\
&\quad + (d_n + d_n^\dagger)]/\sqrt{2}, \\
P_{d_n} - X_{a_n} - X_{c_n} &= -[i(d_n - d_n^\dagger) \\
&\quad + (a_n + a_n^\dagger) + (c_n + c_n^\dagger)]/\sqrt{2}.
\end{aligned} \tag{13}$$

Introducing four independent combined modes by the unitary transformation

$$\begin{pmatrix} \bar{A}_n \\ \bar{B}_n \\ \bar{C}_n \\ \bar{D}_n \end{pmatrix} = \begin{pmatrix} \frac{i}{\sqrt{3}} & \frac{1}{\sqrt{3}} & 0 & \frac{1}{\sqrt{3}} \\ \frac{1}{\sqrt{3}} & \frac{i}{\sqrt{3}} & \frac{1}{\sqrt{3}} & 0 \\ -\frac{2i}{\sqrt{15}} & \frac{1}{\sqrt{15}} & i\sqrt{\frac{3}{5}} & \frac{1}{\sqrt{15}} \\ \frac{1}{\sqrt{15}} & -\frac{2i}{\sqrt{15}} & \frac{1}{\sqrt{15}} & i\sqrt{\frac{3}{5}} \end{pmatrix} \begin{pmatrix} a_n \\ b_n \\ c_n \\ d_n \end{pmatrix} \tag{14}$$

we can rewrite Eqs. (13) as

$$\begin{aligned}
P_{a_n} - X_{b_n} - X_{d_n} &= -\frac{\sqrt{3}}{\sqrt{2}}(\bar{A}_n + \bar{A}_n^\dagger), \\
P_{b_n} - X_{a_n} - X_{c_n} &= -\frac{\sqrt{3}}{\sqrt{2}}(\bar{B}_n + \bar{B}_n^\dagger), \\
P_{c_n} - X_{b_n} - X_{d_n} &= -\frac{\sqrt{5}}{\sqrt{6}}(\bar{C}_n + \bar{C}_n^\dagger) - \frac{2}{\sqrt{6}}(\bar{A}_n + \bar{A}_n^\dagger), \\
P_{d_n} - X_{a_n} - X_{c_n} &= -\frac{\sqrt{5}}{\sqrt{6}}(\bar{D}_n + \bar{D}_n^\dagger) - \frac{2}{\sqrt{6}}(\bar{B}_n + \bar{B}_n^\dagger).
\end{aligned} \tag{15}$$

Therefore, the original modes  $a_n, b_n, c_n, d_n$  will be in a square cluster state if each of the four combined modes defined in Eq. (14) is in a single-mode amplitude squeezed state.

For a T-type cluster state of the four modes  $a_n, b_n, c_n, d_n$  of the  $n$ th resonators of the arrays, as shown in Fig. 3(c), we consider the amplitude combinations

$$\begin{aligned}
P_{b_n} - X_{a_n} - X_{c_n} - X_{d_n} &= -[i(b_n - b_n^\dagger) + (a_n + a_n^\dagger) \\
&\quad + (c_n + c_n^\dagger) + (d_n + d_n^\dagger)]/\sqrt{2}, \\
P_{a_n} - X_{b_n} &= -[i(a_n - a_n^\dagger) + (b_n + b_n^\dagger)]/\sqrt{2}, \\
P_{c_n} - X_{b_n} &= -[i(c_n - c_n^\dagger) + (b_n + b_n^\dagger)]/\sqrt{2}, \\
P_{d_n} - X_{b_n} &= -[i(d_n - d_n^\dagger) + (b_n + b_n^\dagger)]/\sqrt{2}.
\end{aligned} \tag{16}$$

Introducing four independent combined modes by the unitary transformation

$$\begin{pmatrix} \bar{A}_n \\ \bar{B}_n \\ \bar{C}_n \\ \bar{D}_n \end{pmatrix} = \begin{pmatrix} \frac{i}{\sqrt{2}} & \frac{1}{\sqrt{2}} & 0 & 0 \\ \frac{1}{2} & \frac{1}{2} & \frac{1}{2} & \frac{1}{2} \\ -\frac{i}{\sqrt{6}} & \frac{1}{\sqrt{6}} & i\sqrt{\frac{2}{3}} & 0 \\ -\frac{i}{2\sqrt{3}} & \frac{1}{2\sqrt{3}} & -\frac{i}{2\sqrt{3}} & \frac{i\sqrt{3}}{2} \end{pmatrix} \begin{pmatrix} a_n \\ b_n \\ c_n \\ d_n \end{pmatrix} \tag{17}$$

we can rewrite Eqs. (16) as

$$\begin{aligned}
P_{a_n} - X_{b_n} &= -(\bar{A}_n + \bar{A}_n^\dagger), \\
P_{b_n} - X_{a_n} - X_{c_n} - X_{d_n} &= -\sqrt{2}(\bar{B}_n + \bar{B}_n^\dagger), \\
P_{c_n} - X_{b_n} &= -\frac{1}{2}(\bar{A}_n + \bar{A}_n^\dagger) - \frac{\sqrt{3}}{2}(\bar{C}_n + \bar{C}_n^\dagger), \\
P_{d_n} - X_{b_n} &= -\frac{2\sqrt{2}}{\sqrt{12}}(\bar{D}_n + \bar{D}_n^\dagger) \\
&\quad - \frac{1}{\sqrt{12}}(\bar{C}_n + \bar{C}_n^\dagger) \\
&\quad - \frac{\sqrt{3}}{\sqrt{12}}(\bar{A}_n + \bar{A}_n^\dagger).
\end{aligned} \tag{18}$$

Therefore, the original modes  $a_n, b_n, c_n, d_n$  will be in a T-type cluster state if each of the four combined modes defined in Eq. (17) is in a single-mode amplitude squeezed state.

Based on the above discussion, it becomes clear that the generation of a CV quadripartite cluster state is equivalent to the preparation of each of four proper linearly combined modes in a single-mode amplitude squeezed state [27]. In the following we will investigate how to engineer an effective Hamiltonian and find a procedure to generate single-mode squeezed states of the combined modes and the cluster states. Since the strategies for the generation of the linear, square, and T-shape cluster states are similar, as an example, here we only discuss the case of preparing a linear cluster state.

First, we work out an effective Hamiltonian for the generation of single-mode squeezed states of the combined modes defined in Eq. (11). By performing the unitary transformation  $U_1(t) = e^{-iH_0t}$  to the Hamiltonian (1), the total Hamiltonian can be changed to

$$\begin{aligned}
H &= \{g_a\sigma_+ e^{i\omega_0 t} (a_1 e^{-i\omega_0 t} + a_1^\dagger e^{i\omega_0 t}) + g_b\sigma_+ e^{i\omega_0 t} \\
&\quad \times (b_1 e^{-i\omega_0 t} + b_1^\dagger e^{i\omega_0 t}) + g_c\sigma_+ e^{i\omega_0 t} (c_1 e^{-i\omega_0 t} + c_1^\dagger e^{i\omega_0 t}) \\
&\quad + g_d\sigma_+ e^{i\omega_0 t} (d_1 e^{-i\omega_0 t} + d_1^\dagger e^{i\omega_0 t}) + \text{H.c.}\} + H_{\text{drive}} + H_2.
\end{aligned} \tag{19}$$

Then another unitary transformation  $U_2(t) = T \exp[-i \int_0^t H_{\text{drive}}(t') dt']$  is applied to the Hamiltonian (19), where  $T$  is the time order operator. If the parameters  $\xi_{\pm, k}$  are sufficiently small, by only keeping the parameter  $\xi_{\pm, k}$  to first order, the first two parts of Eq. (19) can be written as

$$\begin{aligned}
H &= \left\{ \sigma_+ e^{i\omega_0 t} [g_a (a_1 e^{-i\omega_0 t} + a_1^\dagger e^{i\omega_0 t}) + g_b (b_1 e^{-i\omega_0 t} + b_1^\dagger e^{i\omega_0 t}) \right. \\
&\quad \left. + g_c (c_1 e^{-i\omega_0 t} + c_1^\dagger e^{i\omega_0 t}) + g_d (d_1 e^{-i\omega_0 t} + d_1^\dagger e^{i\omega_0 t}) \right]
\end{aligned}$$

$$\begin{aligned} & \times \left( 1 - \sum_j \{ \xi_{+,k} [e^{i(\omega_{+,k}t + \phi_{+,k})} - e^{-i(\omega_{+,k}t + \phi_{+,k})}] \right. \\ & \left. + \xi_{-,k} [e^{i(\omega_{-,k}t + \phi_{-,k})} - e^{-i(\omega_{-,k}t + \phi_{-,k})}] + \text{H.c.} \right) \}. \quad (20) \end{aligned}$$

Choosing the frequencies  $\omega_{+,k} = \omega_0 + \omega_k$  and  $\omega_{-,k} = \omega_0 - \omega_k$  [51] and ignoring the fast oscillation terms in Eq. (20) because of the condition  $\{\omega_k, \omega_0, \omega_{\pm,k}, \omega_k - \omega_{k'}\} \gg g_j$ , we arrive at the effective Hamiltonian

$$\begin{aligned} H^{\text{eff}} = & \{ \sigma_+ [(G_{+,a} e^{-i\phi_{+,a}} a_1^\dagger + G_{-,a} e^{-i\phi_{-,a}} a_1) \\ & + (G_{+,b} e^{-i\phi_{+,b}} b_1^\dagger + G_{-,b} e^{-i\phi_{-,b}} b_1) \\ & + (G_{+,c} e^{-i\phi_{+,c}} c_1^\dagger + G_{-,c} e^{-i\phi_{-,c}} c_1) \\ & + (G_{+,d} e^{-i\phi_{+,d}} d_1^\dagger + G_{-,d} e^{-i\phi_{-,d}} d_1)] + \text{H.c.} \}, \quad (21) \end{aligned}$$

with  $G_{+,k} = \xi_{+,k} g_k$  and  $G_{-,k} = \xi_{-,k} g_k$ .

In the following we will show that the combined modes  $\bar{A}_1, \bar{B}_1, \bar{C}_1, \bar{D}_1$  defined in Eq. (11) can be respectively prepared in single-mode squeezed states by properly choosing the parameters of the effective Hamiltonian (21). Note that the Hamiltonian  $H_2$  is not changed by the above two unitary transformations. Therefore, the generation of cluster states of the modes  $a_1, b_1, c_1, d_1$  of the first four resonators is realized by the first part of the effective Hamiltonian (21) that involves the modes  $a_1, b_1, c_1, d_1$  and the replication of the resulting cluster states in the other resonators is realized by the Hamiltonian  $H_2$ . In terms of the operators of the combined modes defined in Eq. (11), the Hamiltonian  $H_2$  can be expressed in the form

$$\begin{aligned} \bar{H}_2 = & \sum_{n=1}^{N-1} J (\bar{A}_n^\dagger \bar{A}_{n+1} + \bar{B}_n^\dagger \bar{B}_{n+1} + \bar{C}_n^\dagger \bar{C}_{n+1} \\ & + \bar{D}_n^\dagger \bar{D}_{n+1} + \text{H.c.}). \quad (22) \end{aligned}$$

This represents the energy swapping between the modes of the nearest-neighbor resonators  $\alpha_n$  and  $\alpha_{n+1}$  ( $\alpha = \bar{A}, \bar{B}, \bar{C}, \bar{D}$ ).

The generation of the single-mode squeezed states of the four combined modes can be implemented by the following steps. In the first step of preparation, we switch on the  $\sigma_z$  driving fields only to the resonators  $a_1, b_1$  by choosing

$$\begin{aligned} \xi_{\pm,a} = \xi_{\pm,b} = \xi_{\pm}, \\ \xi_{+,c} = \xi_{-,c} = \xi_{+,d} = \xi_{-,d} = 0 \end{aligned} \quad (23)$$

and the phases of the driving fields

$$\phi_{+,a} = \frac{3}{2}\pi, \quad \phi_{-,a} = \frac{1}{2}\pi, \quad \phi_{+,b} = \phi_{-,b} = \pi. \quad (24)$$

Here we have also assumed the coupling constants of the qubit with the superconducting transmission line resonators to be same, i.e.,  $g_a = g_b = g_c = g_d = g$ . Finally, we obtain the effective Hamiltonian

$$\bar{H}_{1,\text{1st}}^{\text{eff}} = \sqrt{2(G_-^2 - G_+^2)} \sigma_+ [\bar{A}_1 \cosh r + \bar{A}_1^\dagger \sinh r] + \text{H.c.}, \quad (25)$$

with  $G_\pm = \xi_\pm g$ ,  $\cosh r = \frac{G_-}{\sqrt{G_-^2 - G_+^2}}$ ,  $\sinh r = \frac{G_+}{\sqrt{G_-^2 - G_+^2}}$ , and  $r = \tanh^{-1} \frac{G_+}{G_-}$ . To make the system to be stable, it is required that  $\xi_+ < \xi_-$ .

The evolution of the system follows the master equation

$$\frac{d}{dt} \bar{\rho} = -i [\bar{H}_{1,\text{1st}}^{\text{eff}} + \bar{H}_2, \bar{\rho}] + \frac{\Gamma}{2} D[\sigma_-] \bar{\rho}. \quad (26)$$

We now apply a unitary transformation  $U = \bigotimes_{n=1}^N S(\bar{A}_n)$  to the master equation (26), where  $S(\alpha_n) = \exp\{(-1)^n \frac{r}{2} [\alpha_n^{\dagger 2} - \alpha_n^2]\}$  is the single-mode squeezing operator of mode  $\alpha_n$ . After the squeezing transformation, the master equation (26) becomes

$$\begin{aligned} \frac{d}{dt} \bar{\rho}' = & -i [\sqrt{2(G_-^2 - G_+^2)} (\sigma_+ \bar{A}_1 + \sigma_- \bar{A}_1^\dagger) \\ & + \bar{H}_2, \bar{\rho}'] + \kappa D[\sigma_-] \bar{\rho}'. \quad (27) \end{aligned}$$

In the squeezing representation, the engineering process of the squeezing states becomes clear. The qubit continually absorb photons from the combined mode  $\bar{A}_1$  and then the absorbed energy leaks out of the system via the decay of the qubit, which is described by  $D[\sigma_-] \bar{\rho}'$ . Meanwhile, other combined modes  $\bar{A}_n$  ( $n \neq 1$ ) are cooled via the swapping interaction  $\bar{H}_2$ . Finally, the qubit is in its ground state and all the combined modes are in the vacuum. The steady state of the whole system is a tensor product of the vacuum state for all the combined modes and the qubit ground state, i.e.,  $|\psi_s\rangle = \bigotimes_{n=1}^N |0_{\bar{A}_n}\rangle \otimes |g\rangle$ . In the original representation, the steady state can be written in the form  $|\psi_s\rangle = \bigotimes_{n=1}^N \exp\{(-1)^n \frac{r}{2} [\bar{A}_n^{\dagger 2} - \bar{A}_n^2]\} |0_{\bar{A}_n}\rangle \otimes |g\rangle$ . Since the remaining modes  $\bar{B}_n, \bar{C}_n, \bar{D}_n$  are decoupled from the modes  $\bar{A}_n$  and the qubit, we suppose that they are in a undetermined state  $\bigotimes_{n=1}^N \rho_{\bar{B}_n, \bar{C}_n, \bar{D}_n}$ . Then the total system is in a state described by the density operator

$$\bar{\rho} = |g\rangle\langle g| \bigotimes_{n=1}^N S(\bar{A}_n) |0_{(\bar{A}_n)}\rangle \langle 0_{(\bar{A}_n)}| S^\dagger(\bar{A}_n) \otimes \rho_{\bar{B}_n, \bar{C}_n, \bar{D}_n}. \quad (28)$$

Now the combined modes  $\bar{A}_n$  have been prepared in the single-mode squeezed states.

In the second step, we turn off the driving fields in the first step and switch on another set of the driving fields to place the combined modes  $\bar{B}_n$  in a single-mode squeezed vacuum state. To this end, we choose the following parameters in the effective Hamiltonian (21):

$$\begin{aligned} \xi_{\pm,a} = \xi_{\pm,b} = \xi_{\pm,c} = \xi_{\pm}, \\ \xi_{\pm,d} = 0 \end{aligned} \quad (29)$$

and the phases of the driving fields

$$\begin{aligned} \phi_{\pm,a} = \phi_{\pm,c} = \pi, \\ \phi_{+,b} = \frac{3}{2}\pi, \quad \phi_{-,b} = \frac{1}{2}\pi, \\ \phi_{\pm,d} = 0. \end{aligned} \quad (30)$$

As a result, we obtain the effective Hamiltonian

$$\bar{H}_{1,\text{2nd}} = \sqrt{3(G_-^2 - G_+^2)} \sigma_+ [\bar{B}_1 \cosh r + \bar{B}_1^\dagger \sinh r] + \text{H.c.} \quad (31)$$

In the third step, we turn off the driving fields in the second step and switch on a set of driving fields to prepare the combined modes  $\bar{C}_n$  in a single-mode squeezed state. For

this purpose, we choose

$$\begin{aligned}\xi_{\pm,a} &= \xi_{\pm,b} = \xi_{\pm}, \\ \xi_{\pm,c} &= \xi_{\pm,d} = 2\xi_{\pm}\end{aligned}\quad (32)$$

and the phases of the driving fields

$$\begin{aligned}\phi_{-,a} &= \phi_{+,c} = \frac{3}{2}\pi, & \phi_{+,a} &= \phi_{-,c} = \frac{1}{2}\pi, \\ \phi_{\pm,b} &= \phi_{\pm,d} = \pi.\end{aligned}\quad (33)$$

The effective Hamiltonian (21) has the form

$$\bar{H}_{1,3rd} = \sqrt{10(G_-^2 - G_+^2)}\sigma_+[\bar{C}_1 \cosh r + \bar{C}_1^\dagger \sinh r] + \text{H.c.}\quad (34)$$

In the final step, we turn off the driving fields in the third step and switch on a set of driving fields to prepare the combined modes  $\bar{D}_n$  in a single-mode squeezed state. For this purpose, we choose the parameters

$$\begin{aligned}\xi_{\pm,a} &= \xi_{\pm,b} = \xi_{\pm}, \\ \xi_{\pm,c} &= 2\xi_{\pm}, \quad \xi_{\pm,d} = 3\xi_{\pm}\end{aligned}\quad (35)$$

and

$$\begin{aligned}\phi_{\pm,a} &= 0, \\ \phi_{+,b} &= \phi_{-,d} = \frac{1}{2}\pi, & \phi_{-,b} &= \phi_{+,d} = \frac{3}{2}\pi, \\ \phi_{+,c} &= \phi_{-,c} = \pi.\end{aligned}\quad (36)$$

In this way, the effective Hamiltonian (21) takes the form

$$\bar{H}_{1,4th} = \sqrt{15(G_-^2 - G_+^2)}\sigma_+[\bar{D}_1 \cosh r + \bar{D}_1^\dagger \sinh r] + \text{H.c.}\quad (37)$$

As shown in the first step, using the effective Hamiltonians (25), (31), (34), and (37), one can respectively prepare the combined modes  $\bar{B}_n, \bar{C}_n, \bar{D}_n$  in a single-mode squeezed state. After these four steps, the whole system is in the state  $|\Psi\rangle_{\text{cluster}} \otimes |g\rangle$ , where  $|\Psi\rangle_{\text{cluster}} = \bigotimes_{n=1}^N S(\bar{A}_n)|0_{\bar{A}_n}\rangle \otimes S(\bar{B}_n)|0_{\bar{B}_n}\rangle \otimes S(\bar{C}_n)|0_{\bar{C}_n}\rangle \otimes S(\bar{D}_n)|0_{\bar{D}_n}\rangle$ .

The variances of quadrature combinations (12) in the state  $|\Psi\rangle_{\text{cluster}}$  are given by

$$\begin{aligned}Vx1 &= V(P_{a_n} - X_{b_n}) = e^{(-1)^n 2r}, \\ Vx2 &= V(P_{b_n} - X_{a_n} - X_{c_n}) = \frac{3}{2}e^{(-1)^n 2r}, \\ Vx3 &= V(P_{c_n} - X_{b_n} - X_{d_n}) = \frac{3}{2}e^{(-1)^n 2r}, \\ Vx4 &= V(P_{d_n} - X_{c_n}) = e^{(-1)^n 2r}.\end{aligned}\quad (38)$$

All four variances tend to zero in the limit of infinite squeezing when  $n$  is an odd number. This means that the first (third, fifth, seventh, and ninth) four resonators of the arrays  $A, B, C, D$  are prepared in a linear CV cluster state.

Note that the variances (38) with an even number  $n$  are divergent when the squeezing approaches infinity. This means that the combined modes  $\bar{A}_n, \bar{B}_n, \bar{C}_n, \bar{D}_n$  with an even number  $n$  are not in an amplitude squeezed state. For the second (fourth, sixth, eighth, and tenth) four resonators of the arrays  $A, B, C, D$ , one should consider the following combinations of

quadrature components:

$$\begin{aligned}X_{a_n} + P_{b_n} &= i(\bar{A}_n - \bar{A}_n^\dagger), \\ X_{b_n} + P_{a_n} + P_{c_n} &= \sqrt{\frac{3}{2}}i(\bar{B}_n - \bar{B}_n^\dagger), \\ X_{c_n} + P_{b_n} + P_{d_n} &= \frac{1}{2}i(\bar{A}_n - \bar{A}_n^\dagger) + \frac{\sqrt{5}}{2}i(\bar{C}_n - \bar{C}_n^\dagger), \\ X_{d_n} + P_{c_n} &= \sqrt{\frac{1}{6}}i(\bar{B}_n - \bar{B}_n^\dagger) + \sqrt{\frac{5}{6}}i(\bar{D}_n - \bar{D}_n^\dagger).\end{aligned}\quad (39)$$

These combinations can be obtained from Eqs. (12) by the canonical transformations  $P \rightarrow X$  and  $X \rightarrow -P$  and also satisfy the definition (7) for a linear cluster state. The variances of the combinations of quadrature components Eqs. (39) in the state  $|\Psi\rangle_{\text{cluster}}$  can be found to be

$$\begin{aligned}Vp1 &= V(X_{a_n} + P_{b_n}) = e^{-2r}, \\ Vp2 &= V(X_{b_n} + P_{a_n} + P_{c_n}) = \frac{3}{2}e^{-2r}, \\ Vp3 &= V(X_{c_n} + P_{b_n} + P_{d_n}) = \frac{3}{2}e^{-2r}, \\ Vp4 &= V(X_{d_n} + P_{c_n}) = e^{-2r}.\end{aligned}\quad (40)$$

When the squeezing gets infinity, all the variances are to be zero. Therefore, the second (fourth, sixth, eighth, and tenth) four resonators of the arrays  $A, B, C, D$  are also in a CV linear cluster state.

To confirm the above scheme, we numerically solve the master equation (26) with the effective Hamiltonians (25), (31), (34), and (37), respectively. Because of the limitation of available numerical calculation capacity, here we only consider the system consisting of eight resonators ( $n = 2$ ) in the numerical simulation. In the present calculation, the system is initially prepared in the state  $|g\rangle \otimes |0_{a_1}, 0_{b_1}, 0_{c_1}, 0_{d_1}\rangle \otimes |0_{a_2}, 0_{b_2}, 0_{c_2}, 0_{d_2}\rangle$ . We assume that the change of the driving fields is sudden. In Figs. 4 and 5, the variances (38) with  $n = 1$  and the variances (40) with  $n = 2$  are shown. It is observed in Fig. 4 that in each of the steps one of the variances (38) rapidly decreases and approaches a constant close to zero. This means that the modes of the first four resonators are definitely brought to a linear cluster state by the decay of the qubit. The relaxation time to the steady state is about  $100/\kappa$ . It is shown in Fig. 5 that when the variances (38) become constant, the variances

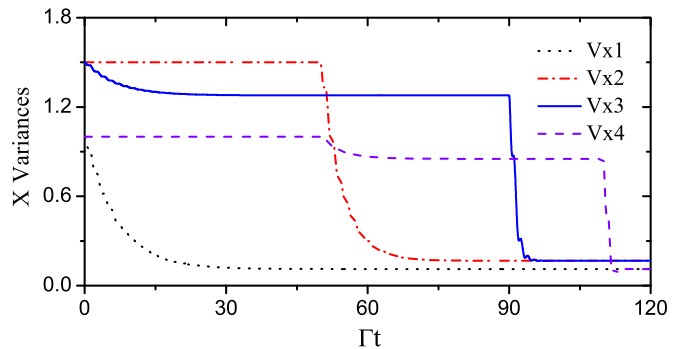


FIG. 4. Time evolution of the variances (38) with  $n = 1$  versus the dimensionless time  $\Gamma t$ . In the calculation, the parameters are chosen as  $g/2\pi = 0.025$  GHz,  $\Gamma/2\pi = 0.02$  GHz,  $J/2\pi = 0.01$  GHz,  $\xi_- = 0.2$ , and  $\xi_+ = 0.16$ .

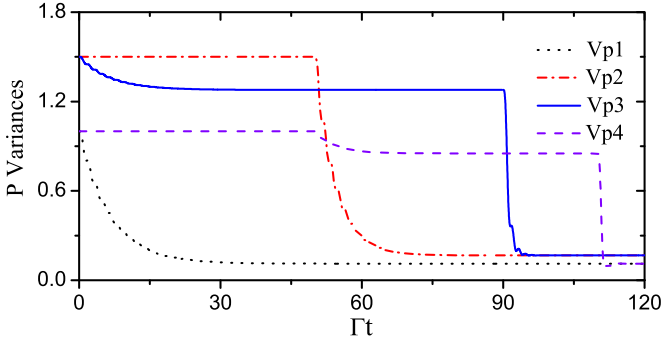


FIG. 5. Time evolution of the variances (40) with  $n = 2$  versus the dimensionless time  $\Gamma t$ . In the calculation, the parameters are chosen as  $g/2\pi = 0.025$  GHz,  $\Gamma/2\pi = 0.02$  GHz,  $J/2\pi = 0.01$  GHz,  $\xi_- = 0.2$ , and  $\xi_+ = 0.16$ .

(40) approach constants close to zero. Thus, the replication of the resulting cluster state in the second four resonators can be completed via the swapping interaction during the generation of the cluster state in the first four resonators. It is also shown in Fig. 4 that the relaxation times to the steady state in each of the steps for the generation of the single-mode squeezed states are different. This phenomenon can be understood by the effective Hamiltonians (25), (31), (34), and (37). One may notice that the coupling strengths between the qubit and the combined mode to be cooled down to a single-mode squeezed state are different in each of the steps, i.e.,  $\sqrt{x(G_-^2 - G_+^2)}$  ( $x = 2, 3, 10, 15$ ). When the coupling strength is large, the energy can be rapidly transferred from the combined mode to the qubit and then the absorbed energy is leaves the resonators via the decay of the qubit. Thus, the larger the effective coupling strength is, the shorter the relaxation time is to the steady state.

#### IV. GENERATION AND REPLICATION OF QUADRIPARTITE GHZ STATES

The GHZ state is also an important multipartite entangled state and has different entanglement properties from the cluster states [22,26]. In this section we investigate how to generate quadripartite GHZ states in the system as shown in Fig. 1.

Consider the four combinations of quadrature components of the fields of the  $n$ -th-column resonators of the arrays  $a, b, c, d$ ,

$$\begin{aligned} X_{a_n} + X_{b_n} + X_{c_n} + X_{d_n} &= [(a_n + a_n^\dagger) + (b_n + b_n^\dagger) \\ &\quad + (c_n + c_n^\dagger) + (d_n + d_n^\dagger)]/\sqrt{2}, \\ P_{a_n} - P_{b_n} &= -[i(a_n - a_n^\dagger) - i(b_n - b_n^\dagger)]/\sqrt{2}, \\ P_{b_n} - P_{c_n} &= -[i(b_n - b_n^\dagger) - i(c_n - c_n^\dagger)]/\sqrt{2}, \\ P_{c_n} - P_{d_n} &= -[i(c_n - c_n^\dagger) - i(d_n - d_n^\dagger)]/\sqrt{2}. \end{aligned} \quad (41)$$

If the variances of these combinations in a state get to zero, the state is said to be a CV GHZ state [23]. We introduce the four

orthogonal combined modes by the unitary transformation

$$\begin{pmatrix} \tilde{A}_n \\ \tilde{B}_n \\ \tilde{C}_n \\ \tilde{D}_n \end{pmatrix} = \begin{pmatrix} \frac{1}{2} & \frac{1}{2} & \frac{1}{2} & \frac{1}{2} \\ -\frac{i}{\sqrt{2}} & \frac{i}{\sqrt{2}} & 0 & 0 \\ 0 & 0 & -\frac{i}{\sqrt{2}} & \frac{i}{\sqrt{2}} \\ -\frac{i}{2} & -\frac{i}{2} & \frac{i}{2} & \frac{i}{2} \end{pmatrix} \begin{pmatrix} a_n \\ b_n \\ c_n \\ d_n \end{pmatrix}. \quad (42)$$

In terms of these combined annihilation operators and their Hermitian conjugates, the combinations of quadrature components (41) can be rewritten as

$$\begin{aligned} X_{a_n} + X_{b_n} + X_{c_n} + X_{d_n} &= \sqrt{2}(\tilde{A}_n + \tilde{A}_n^\dagger), \\ P_{a_n} - P_{b_n} &= \tilde{B}_n + \tilde{B}_n^\dagger, \\ P_{b_n} - P_{c_n} &= -\frac{1}{2}(\tilde{B}_n + \tilde{B}_n^\dagger) - \frac{1}{2}(\tilde{C}_n + \tilde{C}_n^\dagger) \\ &\quad + \frac{1}{\sqrt{2}}(\tilde{D}_n + \tilde{D}_n^\dagger), \\ P_{c_n} - P_{d_n} &= \tilde{C}_n + \tilde{C}_n^\dagger. \end{aligned} \quad (43)$$

Therefore, the modes  $a_n, b_n, c_n, d_n$  are in a CV GHZ state if each of the combined modes  $\tilde{A}_n, \tilde{B}_n, \tilde{C}_n, \tilde{D}_n$  is in a single-mode amplitude squeezed state. In the following we show how to engineer the effective Hamiltonian to generate these single-mode squeezed states by switching on or off suitable sets of the driving fields.

In terms of the annihilation operators defined in Eq. (42) and their Hermitian conjugates, the Hamiltonian  $H_2$  can be written as

$$\begin{aligned} \tilde{H}_2 &= \sum_{n=1}^{N-1} J(\tilde{A}_n^\dagger \tilde{A}_{n+1} + \tilde{B}_n^\dagger \tilde{B}_{n+1} + \tilde{C}_n^\dagger \tilde{C}_{n+1} \\ &\quad + \tilde{D}_n^\dagger \tilde{D}_{n+1} + \text{H.c.}). \end{aligned} \quad (44)$$

Therefore, the Hamiltonian  $H_2$  keeps the same form as expressed in the operators of the original modes.

Now we try to find a process for putting the four modes  $\tilde{A}_n, \tilde{B}_n, \tilde{C}_n, \tilde{D}_n$  in single-mode squeezed states. Similar to the generation of cluster states in the previous section, the whole process is composed of four steps. In the first step of preparation, we choose the parameters

$$\xi_{\pm,a} = \xi_{\pm,b} = \xi_{\pm,c} = \xi_{\pm,d} = \xi_{\pm} \quad (45)$$

and the phases of the driving fields

$$\phi_{\pm,a} = \phi_{\pm,b} = \phi_{\pm,c} = \phi_{\pm,d} = 0. \quad (46)$$

As a result, the Hamiltonian (21) becomes

$$\tilde{H}_{1,\text{1st}} = 2\sqrt{(G_-^2 - G_+^2)}\sigma_+[\tilde{A}_1 \cosh r + \tilde{A}_1^\dagger \sinh r] + \text{H.c.} \quad (47)$$

In the second step, by choosing the parameters

$$\xi_{\pm,a} = \xi_{\pm,b} = \xi_{\pm}, \quad (48)$$

and the phases of the driving fields

$$\begin{aligned} \phi_{+,a} &= \phi_{-,b} = \frac{3}{2}\pi, \\ \phi_{-,a} &= \phi_{+,b} = \frac{1}{2}\pi. \end{aligned} \quad (49)$$

we obtain the effective Hamiltonian

$$\tilde{H}_{1,2st} = \sqrt{2(G_-^2 - G_+^2)}\sigma_+[\tilde{B}_1 \cosh r + \tilde{B}_1^\dagger \sinh r] + \text{H.c.} \quad (50)$$

In the third step, by choosing the parameters

$$\xi_{\pm,c} = \xi_{\pm,d} = \xi_{\pm} \quad (51)$$

and the phases of the driving fields

$$\begin{aligned} \phi_{+,c} &= \phi_{-,d} = \frac{3}{2}\pi, \\ \phi_{-,c} &= \phi_{+,d} = \frac{1}{2}\pi, \end{aligned} \quad (52)$$

we have the effective Hamiltonian

$$\tilde{H}_{1,3st} = \sqrt{2(G_-^2 - G_+^2)}\sigma_+[\tilde{C}_1 \cosh r + \tilde{C}_1^\dagger \sinh r] + \text{H.c.} \quad (53)$$

In the fourth step, by choosing the parameters

$$\xi_{\pm,a} = \xi_{\pm,b} = \xi_{\pm,c} = \xi_{\pm,d} = \xi_{\pm} \quad (54)$$

and the phases of the driving fields

$$\begin{aligned} \phi_{+,a} &= \phi_{+,b} = \phi_{-,c} = \phi_{-,d} = \frac{3}{2}\pi, \\ \phi_{-,a} &= \phi_{-,b} = \phi_{+,c} = \phi_{+,d} = \frac{1}{2}\pi, \end{aligned} \quad (55)$$

we have the effective Hamiltonian

$$\tilde{H}_{1,4st} = 2\sqrt{(G_-^2 - G_+^2)}\sigma_+[\tilde{D}_1 \cosh r + \tilde{D}_1^\dagger \sinh r] + \text{H.c.} \quad (56)$$

Substituting the effective Hamiltonians (47), (50), (53), and (56) into the master equation (26) and following the same procedure as discussed in the previous section, one can easily show that the combined modes  $\tilde{A}_n, \tilde{B}_n, \tilde{C}_n, \tilde{D}_n$  can be respectively prepared in a single-mode squeezed state via the decay of the qubit and the swapping interaction between the nearest neighbors of the resonators. After the four steps, the system is prepared in the state  $|\tilde{\Psi}\rangle_{\text{GHZ}} = \bigotimes_{n=1}^N S(\tilde{A}_n)|0_{\tilde{A}_n}\rangle \otimes S(\tilde{B}_n)|0_{\tilde{B}_n}\rangle \otimes S(\tilde{C}_n)|0_{\tilde{C}_n}\rangle \otimes S(\tilde{D}_n)|0_{\tilde{D}_n}\rangle$ . In terms of the original operators, the resulting state  $|\Psi\rangle_{\text{GHZ}} = \exp\{(-1)^n \frac{r}{4}[a_n^2 + b_n^2 + c_n^2 + d_n^2 - 2a_n b_n - 2a_n c_n - 2a_n d_n - 2b_n c_n - 2b_n d_n - 2c_n d_n] - \text{H.c.}\}$ . The variances of the combinations of quadrature components (43) in the state  $|\Psi\rangle_{\text{GHZ}}$  are given by

$$\begin{aligned} Vx1 &= V(X_{a_n} + X_{b_n} + X_{c_n} + X_{d_n}) = 2e^{(-1)^n 2r}, \\ Vx2 &= V(P_{a_n} - P_{b_n}) = e^{(-1)^n 2r}, \\ Vx3 &= V(P_{b_n} - P_{c_n}) = e^{(-1)^n 2r}, \\ Vx4 &= V(P_{c_n} - P_{d_n}) = e^{(-1)^n 2r}. \end{aligned} \quad (57)$$

It is clear that all the variances get to zero in the limit of infinite squeezing if  $n$  is odd. This means that the first (third, fifth, seventh, and ninth) four resonators of the arrays  $a, b, c, d$  are prepared in a CV GHZ state.

For the second (fourth, sixth, eighth, and tenth) four resonators, one should consider the combinations of quadrature components

$$\begin{aligned} P_{a_n} + P_{b_n} + P_{c_n} + P_{d_n} &= -i\sqrt{2}(\tilde{A}_n - \tilde{A}_n^\dagger), \\ X_{a_n} - X_{b_n} &= i(\tilde{B}_n - \tilde{B}_n^\dagger), \end{aligned}$$

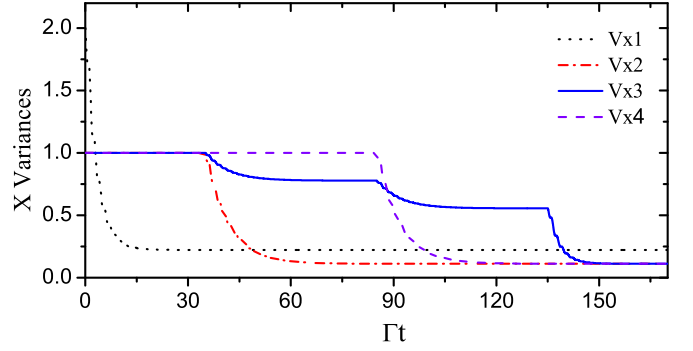


FIG. 6. Time evolution of the variances (57) with  $n = 1$  versus the dimensionless time  $\Gamma t$ . The parameters are chosen as  $g/2\pi = 0.025$  GHz,  $\Gamma/2\pi = 0.02$  GHz,  $J/2\pi = 0.01$  GHz,  $\xi_- = 0.2$ , and  $\xi_+ = 0.16$ .

$$\begin{aligned} X_{b_n} - X_{c_n} &= -\frac{i}{2}(\tilde{B}_n - \tilde{B}_n^\dagger) - \frac{i}{2}(\tilde{C}_n - \tilde{C}_n^\dagger) \\ &\quad + \frac{i}{\sqrt{2}}(\tilde{D}_n - \tilde{D}_n^\dagger), \\ X_{c_n} - X_{d_n} &= i(\tilde{C}_n - \tilde{C}_n^\dagger). \end{aligned} \quad (58)$$

The variances of these combinations in the state  $|\Psi\rangle_{\text{GHZ}}$  are

$$\begin{aligned} Vp1 &= V(P_{a_n} + P_{b_n} + P_{c_n} + P_{d_n}) = 2e^{-2r}, \\ Vp2 &= V(X_{a_n} - X_{b_n}) = e^{-2r}, \\ Vp3 &= V(X_{b_n} - X_{c_n}) = e^{-2r}, \\ Vp4 &= V(X_{c_n} - X_{d_n}) = e^{-2r}. \end{aligned} \quad (59)$$

It is obvious that all these variances tend to zero in the limit  $r \rightarrow \infty$ . Thus, the second (fourth, sixth, eighth, and tenth) four resonators of the arrays  $a, b, c, d$  are also in a CV GHZ state, where each of the combined modes (42) is in a single-mode phase squeezed state.

With the effective Hamiltonians (47), (50), (53), and (56), we solve the master equation (26) and numerically simulate the four-step generation of the CV GHZ states. In Figs. 6 and 7 we plot the time evolution of the variances (38) and (40) versus the dimensionless time  $\kappa t$ . It is shown in Figs. 6 and 7 that one of the variances of the combinations of the quadrature amplitudes can be rapidly reduced to a constant close to zero

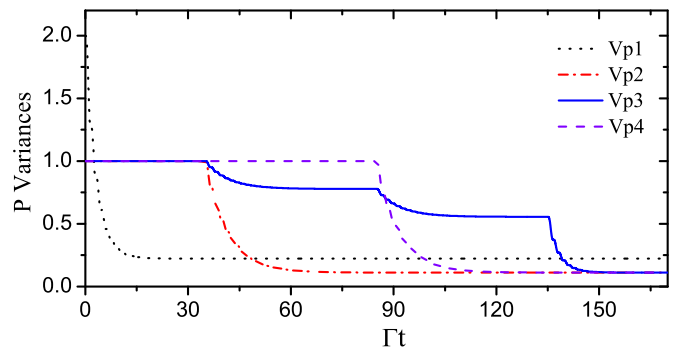


FIG. 7. Time evolution of the variances (59) with  $n = 2$  versus the dimensionless time  $\Gamma t$ . The parameters are chosen as  $g/2\pi = 0.025$  GHz,  $\Gamma/2\pi = 0.02$  GHz,  $J/2\pi = 0.01$  GHz,  $\xi_- = 0.2$ , and  $\xi_+ = 0.16$ .



in each of the four steps. Thus, after the four steps, all the combined modes are prepared in single-mode squeezed states and the original modes of the resonators are in the CV GHZ state. Note that the first four resonators and the second four resonators enter the CV GHZ states at the same time scale.

## V. DISCUSSION AND SUMMARY

We considered a system composed of a gap-tunable superconducting qubit and four chains of linearly coupled superconducting transmission line resonators. The first four resonators of the chains are simultaneously coupled to the qubit. By periodically modulating the transition frequency of the qubit, both the parametric down-conversion-like and the beam-splitter-like interactions between the qubit and the resonators can be realized. In this way, we showed that quadripartite cluster states and GHZ states of the cavity fields of the first four column resonators can be achieved via the decay process of the qubit to its ground state. Moreover, the resulting cluster states and GHZ states can be replicated among the whole chains via the nearest-neighbor swapping interaction of the resonators. This result means that one can generate a set of the cluster states, each of which contains the four resonators from the different chains. Specifically, it is noted that the first-, third-, fifth-, and seventh-column resonators and the second-, fourth-, sixth-, and eighth-column resonators in the chains are in two complementary cluster states, that is, one set of the combination of quadrature components is in a single-mode amplitude squeezed state but the other set of the combination of quadrature components is in a single-mode phase squeezed state. The whole generation and replication process is made up of four steps; in each step one of the four orthogonal combination modes of the resonators is cooled down to a single-mode squeezed state. The four steps are implemented by simply adjusting the driving parameters of the qubit.

Now let us briefly discuss the experimental feasibility of the present scheme. Our numerical simulation shows that the CV cluster states and the CV GHZ states can be achieved within the operation time about  $100/\Gamma$ . To avoid the disturbance of dissipation of resonators, the coherence time of resonators ( $1/\kappa$ , where  $\kappa$  is the damping rate of resonators) must be longer than the operation time, for example, by two orders of magnitude, i.e.,  $1/\kappa \geq 10^4/\Gamma$ . The present scheme needs a bad qubit with a large decay rate  $\Gamma$ , which can be realized by coupling it to an extra relaxation channel [51,52]. For  $\Gamma/2\pi = 0.05$  GHz, the damping rate of resonators should satisfy  $\kappa/2\pi \leq 5.0 \times 10^{-6}$  GHz. Thus, for a frequency of the resonators  $\omega/2\pi = 5.0$  GHz, the present scheme requires the quality factor of resonators  $Q = \omega/\kappa = 10^6$ . In current

experiments, actually, the planar superconducting resonator with a quality factor  $Q$  above  $10^7$  has been realized [53]. On the other hand, the values of the coupling strengths required for the present scheme ( $J/2\pi \sim 0.01$  GHz) are also accessible in the current experiments of superconducting quantum circuits [54]. Therefore, we believe that the present scheme is accessible with current technologies.

Another important issue is how long the resonator chain is accessible with current technologies. For the first four end resonators that are directly coupled to the gap-tunable qubit, we have shown that the resonators can be prepared in the cluster states by four steps, each of which cools down one of the combined modes into a single-mode squeezed state with the assistance of dissipation of the qubit. The four steps are completed within a time scale  $4/\Gamma$ , where  $\Gamma$  is the decay rate of the qubit. The other resonators are prepared in cluster states via the nearest-neighbor interaction of the resonators, i.e., the photon hopping process. If there were no photon loss processes, therefore, the replication mechanism of the cluster states would be scale-free and independent of the length of the arrays and one could build a cluster state chain with an infinite length. In practical situations, however, the length of the resonator chain is limited due to the photon loss of the resonators. The photon hopping time for each of the combined modes is about  $1/J$ , where  $J$  is the swapping interaction strength between the resonators. For each of the cluster states, one needs to replicate the four combined modes. Therefore, the hopping time of one cluster state is about  $4/J$ . On the other hand, the replication of cluster states among the resonators must be completed within the coherence time of resonators  $1/\kappa$ . Thus, the resonator chain length can be roughly estimated to be  $J/4\kappa$ . With the current feasible experiment technique,  $J/2\pi \sim 0.01$  GHz and, estimated as above, the decay rate  $\kappa/2\pi$  of transmission line resonators should be  $5.0 \times 10^{-6}$  GHz. Therefore, the number of resonators that could be prepared in cluster states is limited to be about the order of 100.

Finally, we should point out that the present setup can be directly extended to one including more resonator chains. Thus, we believe that the present investigation may open an approach for the realization of large-scale one-way quantum computing.

## ACKNOWLEDGMENT

This work was supported by the National Natural Science Foundation of China (Grants No. 11374239 and No. 11534008).

- 
- [1] A. Furusawa, J. L. Sørensen, S. L. Braunstein, C. A. Fuchs, H. J. Kimble, and E. S. Polzik, *Science* **282**, 706 (1998).  
 [2] H. Yonezawa, T. Aoki, and A. Furusawa, *Nature (London)* **431**, 430 (2004).  
 [3] S. L. Braunstein and H. J. Kimble, *Phys. Rev. A* **61**, 042302 (2000).

- [4] X. Y. Li, Q. Pan, J. T. Jing, J. Zhang, C. D. Xie, and K. Peng, *Phys. Rev. Lett.* **88**, 047904 (2002).  
 [5] A. Rauschenbeutel, G. Nogues, S. Osngahi, P. Bertet, M. Brune, J. M. Raimond, and S. Haroche, *Science* **288**, 2024 (2000).  
 [6] K. C. Lee, M. R. Sprague, B. J. Sussman, J. Nunn, N. K. Langford, X. M. Jin, T. Champion, P. Michelberger, K. F. Reim,

- D. England, D. Jaksch, and I. A. Walmsley, *Science* **334**, 1253 (2011).
- [7] T. Monz, P. Schindler, J. T. Barreiro, M. Chwalla, D. Nigg, W. A. Coish, M. Harlander, W. Hänsel, M. Hennrich, and R. Blatt, *Phys. Rev. Lett.* **106**, 130506 (2011).
- [8] D. Kielpinski, V. Meyer, M. A. Rowe, C. A. Sackett, W. M. Itano, C. Monroe, and D. J. Wineland, *Science* **291**, 1013 (2001).
- [9] C. F. Roos, M. Riebe, H. Häffner, W. Hänsel, J. Benhelm, G. P. T. Lancaster, C. Becher, F. S. Kaler, and R. Blatt, *Science* **304**, 1478 (2004).
- [10] W. B. Gao, C. Y. Lu, X. C. Yao, P. Xu, O. Gühne, A. Goebel, Y. A. Chen, C. Z. Peng, Z. B. Chen, and J. W. Pan, *Nat. Phys.* **6**, 331 (2010).
- [11] Z. Y. Ou, S. F. Pereira, H. J. Kimble, and K. C. Peng, *Phys. Rev. Lett.* **68**, 3663 (1992).
- [12] S. L. Braunstein and P. van Loock, *Rev. Mod. Phys.* **77**, 513 (2005).
- [13] R. Simon, *Phys. Rev. Lett.* **84**, 2726 (2000).
- [14] L.-M. Duan, G. Giedke, J. I. Cirac, and P. Zoller, *Phys. Rev. Lett.* **84**, 2722 (2000).
- [15] L. Tian, *Phys. Rev. Lett.* **110**, 233602 (2013).
- [16] X.-Y. Lü and J. Wu, *Phys. Rev. A* **82**, 012323 (2010).
- [17] Z.-q. Yin and Y.-J. Han, *Phys. Rev. A* **79**, 024301 (2009).
- [18] P.-B. Li, S.-Y. Gao, and F.-L. Li, *Phys. Rev. A* **88**, 043802 (2013).
- [19] S.-L. Ma, Z. Li, P.-B. Li, and F.-L. Li, *Phys. Rev. A* **90**, 043810 (2014).
- [20] S.-L. Ma, Z. Li, A.-P. Fang, P.-B. Li, S.-Y. Gao, and F.-L. Li, *Phys. Rev. A* **90**, 062342 (2014).
- [21] Z. Li, S.-l. Ma, and F.-l. Li, *Phys. Rev. A* **92**, 023856 (2015).
- [22] P. van Loock and S. L. Braunstein, *Phys. Rev. Lett.* **84**, 3482 (2000).
- [23] P. van Loock and A. Furusawa, *Phys. Rev. A* **67**, 052315 (2003).
- [24] X. L. Su, A. H. Tan, X. J. Jia, J. Zhang, C. D. Xie, and K. C. Peng, *Phys. Rev. Lett.* **98**, 070502 (2007).
- [25] J. T. Jing, J. Zhang, Y. Yan, F. G. Zhao, C. D. Xie, and K. C. Peng, *Phys. Rev. Lett.* **90**, 167903 (2003).
- [26] J. Zhang and S. L. Braunstein, *Phys. Rev. A* **73**, 032318 (2006); J. Zhang, *ibid.* **78**, 034301 (2008).
- [27] M. Yukawa, R. Ukai, P. van Loock, and A. Furusawa, *Phys. Rev. A* **78**, 012301 (2008).
- [28] G.-x. Li, S.-s. Ke, and Z. Ficek, *Phys. Rev. A* **79**, 033827 (2009).
- [29] L.-h. Sun, and G.-x. Li, *Phys. Rev. A* **85**, 065801 (2012).
- [30] P. Wang, M. Chen, N. C. Menicucci, and O. Pfister, *Phys. Rev. A* **90**, 032325 (2014).
- [31] H. J. Briegel and R. Raussendorf, *Phys. Rev. Lett.* **86**, 910 (2001).
- [32] R. Raussendorf and H. J. Briegel, *Phys. Rev. Lett.* **86**, 5188 (2001).
- [33] N. C. Menicucci, P. van Loock, M. Gu, C. Weedbrook, T. C. Ralph, and M. A. Nielsen, *Phys. Rev. Lett.* **97**, 110501 (2006).
- [34] R. J. Schoelkopf and S. M. Girvin, *Nature (London)* **451**, 664 (2008).
- [35] J. Clarke and F. K. Wilhelm, *Nature (London)* **453**, 1031 (2008).
- [36] J. Q. You and F. Nori, *Phys. Today* **58** (11), 42 (2005).
- [37] Y. Makhlin, G. Schon, and A. Shnirman, *Rev. Mod. Phys.* **73**, 357 (2001).
- [38] A. Blais, R.-S. Huang, A. Wallraff, S. M. Girvin, and R. J. Schoelkopf, *Phys. Rev. A* **69**, 062320 (2004).
- [39] C. P. Yang, Q. P. Su, S. B. Zheng, and S. Y. Han, *Phys. Rev. A* **87**, 022320 (2013).
- [40] C.-P. Yang, Q.-P. Su, and F. Nori, *New J. Phys.* **15**, 115003 (2013).
- [41] C.-P. Yang, Q.-P. Su, S.-B. Zheng, and S. Han, *Phys. Rev. B* **92**, 054509 (2015).
- [42] H. Wang, M. Mariantoni, R. C. Bialczak, M. Lenander, E. Lucero, M. Neeley, A. D. O'Connell, D. Sank, M. Weides, J. Wenner, T. Yamamoto, Y. Yin, J. Zhao, J. M. Martinis, and A. N. Cleland, *Phys. Rev. Lett.* **106**, 060401 (2011).
- [43] C.-P. Yang, Q.-P. Su, S.-B. Zheng, and F. Nori, *New J. Phys.* **18**, 013025 (2016).
- [44] C.-P. Yang, S.-B. Zheng, and F. Nori, *Phys. Rev. A* **82**, 062326 (2010).
- [45] F. Quijandría, D. Porras, J. J. García-Ripoll, and D. Zueco, *Phys. Rev. Lett.* **111**, 073602 (2013).
- [46] M. J. Schwarz, J. Goetz, Z. Jiang, T. Niemczyk, F. Deppe, A. Marx, and R. Gross, *New J. Phys.* **15**, 045001 (2013).
- [47] A. Wallraff, D. I. Schuster, A. Blais, J. M. Gambetta, J. Schreier, L. Frunzio, M. H. Devoret, S. M. Girvin, and R. J. Schoelkopf, *Phys. Rev. Lett.* **99**, 050501 (2007).
- [48] P. J. Leek, S. Filipp, P. Maurer, M. Baur, R. Bianchetti, J. M. Fink, M. Göppl, L. Steffen, and A. Wallraff, *Phys. Rev. B* **79**, 180511(R) (2009).
- [49] F. G. Paauw, A. Fedorov, C. J. P. M. Harmans, and J. E. Mooij, *Phys. Rev. Lett.* **102**, 090501 (2009).
- [50] Z. L. Xiang, S. Ashhab, J. Q. You, and F. Nori, *Rev. Mod. Phys.* **85**, 623 (2013).
- [51] D. Porras and J. J. Garcia-Ripoll, *Phys. Rev. Lett.* **108**, 043602 (2012).
- [52] S. L. Ma *et al.*, *Europhys. Lett.* **110**, 40004 (2015).
- [53] A. Megrant *et al.*, *Appl. Phys. Lett.* **100**, 113510 (2012).
- [54] D. L. Underwood, W. E. Shanks, J. Koch, and A. A. Houck, *Phys. Rev. A* **86**, 023837 (2012).